

Geocenter motions from GPS: A unified observation model

David A. Lavallée,¹ Tonie van Dam,² Geoffrey Blewitt,^{3,4} and Peter J. Clarke¹

Received 15 April 2005; revised 22 December 2005; accepted 4 January 2006; published 6 May 2006.

[1] We test a unified observation model for estimating surface-loading-induced geocenter motion using GPS. In principle, this model is more complete than current methods, since both the translation and deformation of the network are modeled in a frame at the center of mass of the entire Earth system. Real and synthetic data for six different GPS analyses over the period 1997.25–2004.25 are used to (1) build a comprehensive appraisal of the errors and (2) compare this unified approach with the alternatives. The network shift approach is found to perform particularly poorly with GPS. Furthermore, erroneously estimating additional scale changes with this approach can suggest an apparently significant seasonal variation which is due to real loading. An alternative to the network shift approach involves modeling degree-1 and possibly higher-degree deformations of the solid Earth in a realization of the center of figure frame. This approach is shown to be more robust for unevenly distributed networks. We find that a unified approach gives the lowest formal error of geocenter motion, smaller differences from the true value when using synthetic data, the best agreement between five different GPS analyses, and the closest (submillimeter) agreement with the geocenter motion predicted from loading models and estimated using satellite laser ranging. For five different GPS analyses, best estimates of annual geocenter motion have a weighted root-mean-square agreement of 0.6, 0.6, and 0.8 mm in amplitude and 21°, 22°, and 22° in phase for x , y , and z , respectively.

Citation: Lavallée, D. A., T. van Dam, G. Blewitt, and P. J. Clarke (2006), Geocenter motions from GPS: A unified observation model, *J. Geophys. Res.*, **111**, B05405, doi:10.1029/2005JB003784.

1. Introduction

[2] The mass contained in the Earth's fluid envelope (**oceans, atmosphere, and continental water**) is constant at human timescales. However, its distribution over the surface of the Earth changes continually. Much of this geographic redistribution of surface mass happens periodically at 24 hour to annual periods and is related to the rotation of the Earth on its axis (e.g., thermally driven atmospheric tides) as well as motion of the Earth around the Sun (e.g., annual global water cycle). In the absence of external forces the center of mass of the entire solid Earth and load system (**CM**) is a fixed point in space; relative to this point a change in the location of the center of mass of the surface load must (by conservation of linear momentum) induce a change in the relative location of the center of mass of the solid Earth (**CE**). This “geocenter motion” causes a detectable translation of a geodetic network attached to the solid Earth,

relative to the center of satellite orbits, which is CM [Chen et al., 1999; Watkins and Eanes, 1993; Watkins and Eanes, 1997]. While geocenter motion is principally a product of mass balance relations, the geodetic network is located on the surface of the solid Earth which also deforms because of redistribution of the load. Thus the same process (redistribution of surface mass) is expressed in the geodetic network in two quite different ways: displacement of the Earth's center related to mass balance and subsequent deformation of the solid Earth due to the load. For a totally rigid Earth, there would be no deformation; in an elastic Earth the deformational movement at a point can reach up to 40% of the magnitude of the geocenter trajectory and must be taken into account [Blewitt, 2003]. A graphical representation of these concepts is given in Figure 1.

[3] Estimates of geocenter motion from space geodesy are important since they fundamentally relate to how we realize the terrestrial reference frame [Blewitt, 2003; Dong et al., 2003]. Conventionally, the center of the International Terrestrial Reference Frame (ITRF) is defined to be at the center of mass of the entire Earth system, i.e., CM [McCarthy and Petit, 2004]. Estimates of geocenter motion can also help to constrain models involving global redistribution of mass [Chen et al., 1999; Cretaux et al., 2002; Dong et al., 1997] and sea level [Blewitt and Clarke, 2003], since they are directly related to the degree-1 component of the surface mass load. This is particularly relevant because current estimates of the degree-1 surface mass load derived

¹School of Civil Engineering and Geosciences, University of Newcastle upon Tyne, Newcastle, UK.

²European Center for Geodynamics and Seismology, Walferdange, Luxembourg.

³Nevada Bureau of Mines and Geology, University of Nevada, Reno, Nevada, USA.

⁴Also at Nevada Seismological Laboratory, University of Nevada, Reno, Nevada, USA.

from environmental models disagree. A number of authors estimate the annual and semiannual components of geocenter motion induced by different models of surface mass redistribution [Bouillé et al., 2000; Chen et al., 1999; Cretaux et al., 2002; Dong et al., 1997; Moore and Wang, 2003]. While the geocenter motions from different atmospheric mass models tend to agree for all components, significant differences (up to 50%) are observed in annual and semiannual geocenter motion from ocean bottom pressure and, more importantly, from continental water mass. The standard deviation about the mean of the modeled annual geocenter from 11 different model combinations [Bouillé et al., 2000; Chen et al., 1999; Cretaux et al., 2002; Dong et al., 1997; Moore and Wang, 2003] suggests the precision of the modeled annual geocenter variation is on the order of ~ 1 mm in amplitude and $\sim 20^\circ$ in phase.

[4] The Gravity Recovery and Climate Experiment (GRACE) mission results [Tapley et al., 2004] will provide significant new information on the surface mass variations over the Earth down to periods of 1 month. However, the GRACE products do not include degree 1 to which GRACE is insensitive. The determination of degree-1 coefficients of the Earth's surface mass load from observational data and the discrimination of modeled environmental data sets is therefore left to other geodetic techniques such as satellite laser ranging (SLR), Doppler orbitography and radiopositioning integrated by satellite (DORIS) and the Global Positioning System (GPS).

[5] It should be noted that no geodetic estimates of secular geocenter motion currently exist; tectonic deformation will produce a net translation of the center of surface figure (CF) relative to the center of mass (CM) which is generally first removed by estimating tectonic velocities at each site. Only if a plate rotation model is used can such an estimate be made and so far is considered systematic reference frame error rather than physical signal [Argus et al., 1999], much further work is required to solve this important reference frame issue. In this work the estimation is considered for the more common use of the term "geocenter motion," that is, assuming tectonic deformation has been first removed. This work does not reflect the ability of a network shift or Helmert transformation approach to resolve the aforementioned reference frame issues associated with what might be called secular "geocenter motion" or even its ability to resolve secular differences between reference frames.

[6] There have been a number of different approaches to estimating geocenter motions from geodetic measurements [Ray, 1999] including (1) the so-called "network shift approach" [Blewitt et al., 1992; Dong et al., 2003; Heflin and Watkins, 1999], also called the "geometric approach" [Cheng, 1999; Pavlis, 1999], which directly models the translation between coordinate frames, (2) the "dynamic approach" [Chen et al., 1999; Pavlis, 1999; Vigue et al., 1992], which estimates degree-1 coefficients of the geopotential, and (3) the "degree-1 deformation" approach [Blewitt et al., 2001; Dong et al., 2003], which equates solid Earth deformation caused by the load to geocenter motion. The dynamic and network shift approach are equivalent (where constraints are minimal), and in this work we only consider the latter. We note that describing the "network shift approach" as "geometric" is misleading

because this approach principally depends on satellite dynamics to locate the Earth center of mass and so is fundamentally a dynamic approach. Here we are consistent with the terminology of Dong et al. [2003]. Lavallée and Blewitt [2002] show that even the nonsatellite technique of very long baseline interferometry (VLBI) is sensitive to geocenter motions via the degree-1 deformation. However, to quote Boucher and Sillard [1999], commenting on the geocenter series submitted to the 1999 International Earth Rotation Service (IERS) analysis campaign to investigate motions of the geocenter, "It appears that, even if Space Geodesy geocenter estimates are sensitive to seasonal variations, the determinations are not yet accurate and reliable enough to adopt an empirical model that would represent a real signal." Disagreement between different geodetic analyses is still considerably larger than that between loading models. Much of this disagreement comes from differences between GPS analyses; estimates from SLR tracking of LAGEOS 1 and 2 [Bouillé et al., 2000; Chen et al., 1999; Cretaux et al., 2002; Moore and Wang, 2003] are in much better agreement.

[7] The source of the disagreement between GPS analyses has been difficult to track down; Dong et al. [2002] and Wu et al. [2002] estimate the size of the error in the network shift approach due to an imperfect network, and Wu et al. [2002] estimate aliasing errors in the degree-1 deformation approach. A number of authors [Blewitt, 2003; Dong et al., 2003; Wu et al., 2002] state that the network shift approach is biased by deficiencies in GPS orbit modeling but a quantitative consideration of how all errors trades off against each other for different networks and approaches has not been completed. Although Dong et al. [2003] suggest the degree-1 deformation approach produces more stable geocenter estimates, Wu et al. [2002] suggest the ignored higher degrees produce a significant error. This uncertainty in how best to estimate geocenter motions from GPS makes it difficult to recommend procedures for defining the terrestrial reference frame [Ray et al., 2004] or make robust inferences about degree-1 surface mass loading. Dong et al. [2003] even suggest that given the improved precision of modern geodetic techniques geocenter motions should be included in the definition of the ITRF as estimable parameters.

[8] Current methods to model geocenter motion consider either the translational or the deformation expression of change in the center of mass of the surface load; here we test a model that unifies these two aspects. In principle, this is a better way to model geocenter motions: It is complete, in that all the displacements associated with geocenter motion are modeled, and it is also conventional, such that displacements are modeled in the CM frame. We complete an appraisal of possible errors in the current geocenter motion estimation strategies applied to GPS and make a comparison of the unified approach with these alternatives.

2. Estimating Geocenter Motions From Space Geodesy

[9] For mathematical convenience we define "geocenter motion" in the context of this paper as the 3-D vector displacement $\Delta\mathbf{r}_{\text{CF-CM}}$ of the center of surface figure (CF) of the solid Earth's surface relative to the center of mass

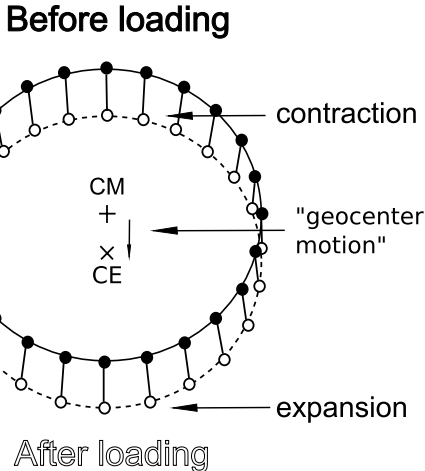


Figure 1. Graphical representation of displacements within a geodetic network due to changing location of center of mass of surface load. CM is center of mass of solid Earth plus load, the origin of satellite orbits which is essentially a kinematic fixed point in space. Two quite different expressions are observed: displacement of center of solid Earth (CE) and deformation of solid Earth.

(CM) of the entire Earth system (solid Earth, oceans, and atmosphere). Although the term “geocenter motions” has been used to describe the vector difference between a number of frames [Blewitt, 2003; Dong *et al.*, 1997], Δr_{CF-CM} or its opposite in sign (Δr_{CM-CF}) are the most commonly estimated geocenter parameters from GPS [Heflin *et al.*, 2002; Malla *et al.*, 1993; Ray, 1999; Vigue *et al.*, 1992], SLR [Bouillé *et al.*, 2000; Chen *et al.*, 1999; Cretaux *et al.*, 2002; Moore and Wang, 2003], and DORIS [Bouillé *et al.*, 2000; Cretaux *et al.*, 2002], so we treat it as the desired estimable parameter. As discussed, the center of mass of the solid Earth (CE) is displaced from CM because of the changing location of the center of mass of the load. CF is a useful point that represents the geometrical center of the Earth’s surface. It is displaced from CE because of the deformation of the solid Earth accompanying loading; if the Earth were rigid, these points would coincide. Since CF is essentially the global average of the surface deformation, it differs in location to CE by only $\sim 2\%$ [Blewitt, 2003]; however, this can be misleading since at specific locations the deformational displacement can be on the order of 40%.

[10] The three-dimensional displacement (east, north, and up) of a point on the Earth’s surface due to surface mass loading can be described [Dziewonski and Anderson, 1981; Farrell, 1972; Lambeck, 1980] using spherical harmonic expansion and a spherically symmetric, layered, nonrotational and isotropic Earth model of the form

$$\begin{aligned} E(\Omega) &= \frac{\rho_s}{\rho_E} \sum_{n=1}^{\infty} \sum_{m=0}^n \sum_{\Phi}^{\{C,S\}} \frac{3l'_n}{(2n+1)} T_{nm}^{\Phi} \frac{\partial_{\lambda} Y_{nm}^{\Phi}(\Omega)}{\cos \varphi} \\ N(\Omega) &= \frac{\rho_s}{\rho_E} \sum_{n=1}^{\infty} \sum_{m=0}^n \sum_{\Phi}^{\{C,S\}} \frac{3l'_n}{(2n+1)} T_{nm}^{\Phi} \partial_{\varphi} Y_{nm}^{\Phi}(\Omega) \\ H(\Omega) &= \frac{\rho_s}{\rho_E} \sum_{n=1}^{\infty} \sum_{m=0}^n \sum_{\Phi}^{\{C,S\}} \frac{3h'_n}{(2n+1)} T_{nm}^{\Phi} Y_{nm}^{\Phi}(\Omega) \end{aligned} \quad (1)$$

where T_{nm}^{Φ} are the spherical harmonic coefficients of the surface load density following the conventions of Blewitt and Clarke [2003] and expressed as the height of a column of seawater, h'_n and l'_n are the degree- n Love numbers which for degree 1 must be specified in our chosen frame [Blewitt, 2003], ρ_s is the density of seawater and ρ_E is the mean density of the Earth.

[11] It can be shown [Trupin *et al.*, 1992] that surface integration of (1) gives the following geocenter motion between the CM and CF frames:

$$\Delta \tilde{r}_{CF-CM} = \left(\frac{([h'_1]_{CE} + 2[l'_1]_{CE})}{3} - 1 \right) \frac{\rho_s}{\rho_E} \begin{pmatrix} T_{11}^C \\ T_{11}^S \\ T_{10}^C \end{pmatrix} \quad (2)$$

We choose to use CE frame Love numbers in (2) since the $\frac{([h'_1]_{CE} + 2[l'_1]_{CE})}{3} - 1$ term helps demonstrate the concept of translation and then deformation of the solid Earth. The unity term is the translation from CM to CE which is much larger than the first term which describes the average deformation of the solid Earth that displaces CF from CE. The first term has a magnitude of 0.021 using the Love numbers of Farrell [1972]; it is important to recall, however, that the deformation at a point given by (1) can be much larger than this.

2.1. A Unified Observation Model

[12] A unified approach for geocenter motion models displacements in the CM frame at each site using (1), where Love numbers are in the CM frame. In this way both the translation and deformation of the network are modeled. Strictly speaking, only the degree-1 deformation need be modeled as the higher degrees do not relate to the center of mass of the load. Higher-degree deformation will, however, be present in geodetic observations and could alias estimates of geocenter motion if not included, so it can be beneficial to include some of them. For short we call this unified model the “CM method.” The design matrix for this approach is given in Appendix A.

[13] A note of caution must be attached to the CM method when anything but a full weight matrix is used during estimation. Estimating the translational aspects of geocenter motions relies on determining the CM frame via simultaneous solution for GPS satellite orbital dynamics and coordinates of a global site network. This information is present in the off diagonal elements of the stochastic model; information on the determination of individual site coordinates relative to the network as a whole is given along the diagonal. It is the stochastic model that determines the relative influence of translation and deformation on the estimate of geocenter motion. If the covariance matrix of observations is diagonal or block diagonal the translation of the network is effectively given a much larger weight than the deformation and the CM method gives identical results to the network shift method.

[14] This is particularly pertinent for GPS results obtained using precise point positioning [Zumberge *et al.*, 1997], in which orbits are fixed (considered perfect in the stochastic

model). While point positioning is a very useful approach for regional analysis, it is generally not suitable for estimating global parameters such as geocenter motion. The results obtained will be identical to those from the network shift approach for a global network and the same as common mode filtering [Wdowinski *et al.*, 1997] on a regional scale. Davis *et al.* [2004] attempt to estimate degree-1 deformation from continental-scale point-positioning results in this manner so that the remaining higher-degree (>1) deformation can be compared to GRACE measurements. However, Davis *et al.* [2004] have removed only a mean from their GPS results (and not the degree-1 deformation), so this is equivalent to common mode filtering on a continental scale.

2.2. The Network Shift Approach

[15] Estimation of $\Delta\mathbf{r}_{\text{CF-CM}}$ from GPS measurements has been most commonly performed by modeling displacements as a translation only [Heflin *et al.*, 2002; Heflin and Watkins, 1999]. Generally, a least squares approach is used to estimate a Helmert transformation with up to seven parameters [Blewitt *et al.*, 1992]. We follow [Dong *et al.*, 2003] in calling this the “network shift approach.” This approach models only the translational aspect of geocenter motion, and it is easy to see how such a procedure could be developed from (2) since the globally averaged deformation is very small. Modeling coordinate displacements as only a translation, however, ignores the quite large deformations that can occur on a site by site basis and the estimate in reality defines a center of network (CN) frame [Wu *et al.*, 2002] giving geocenter motion $\Delta\mathbf{r}_{\text{CN-CM}}$ which is only an approximation of $\Delta\mathbf{r}_{\text{CF-CM}}$.

[16] When estimating a Helmert transformation it can be necessary to estimate rotation parameters since in fiducial-free GPS analysis network orientation is only loosely constrained [Heflin *et al.*, 1992]; however, a scale parameter should not be estimated. A scale parameter is sometimes included when estimating Helmert transformations to investigate any systematic differences in the definition of scale between different techniques, e.g., VLBI, SLR, GPS or DORIS [Altamimi *et al.*, 2002]. When estimating $\Delta\mathbf{r}_{\text{CF-CM}}$, however, there is no reason to include a scale parameter since we are using only one technique and the scale definition is the same. An estimated scale parameter could absorb some of the loading deformation due to an imperfect (e.g., continentally biased) network giving an apparent scale error; this error is unfortunate and can be completely avoided by not estimating scale.

2.3. Degree-1 Deformation Approach

[17] Blewitt *et al.* [2001] estimate the degree-1 coefficients of the surface mass load (expressed as the load mass moment) from GPS using a priori information about the Earth’s elastic properties given by the loading model specified in (1) and the degree-1 Love numbers [Farrell, 1972] in the CF frame. By modeling only the deformation the translational aspect of geocenter motion does not influence the estimate. Blewitt *et al.* [2001] model GPS displacements in a realization of the CF frame with

$$[\Delta\mathbf{s}_i]_{\text{CF}} = \mathbf{G}^T \text{diag} [[l'_1]_{\text{CF}} [l'_1]_{\text{CF}} [h'_1]_{\text{CF}}] \mathbf{G} \frac{\mathbf{m}}{M_{\oplus}} \quad (3)$$

where \mathbf{m} is the “load moment,” $[h'_1]_{\text{CF}}$ and $[l'_1]_{\text{CF}}$ are degree-1 Love numbers in the CF frame, and for simplification the height and lateral degree-1 spherical harmonic functions (1) are identified with the elements of the geocentric to topocentric rotation matrix \mathbf{G} (Appendix A). In the notation of this paper this is identical to (1) for the CF frame where we identify

$$\frac{\mathbf{m}}{M_{\oplus}} = \frac{\rho_s}{\rho_E} \begin{pmatrix} T_{11}^C \\ T_{11}^S \\ T_{10}^C \end{pmatrix} \quad (4)$$

and hence (3) is a method to estimate $\Delta\mathbf{r}_{\text{CF-CM}}$ through (2). [Dong *et al.*, 2003] named this the “degree-1 deformation” approach; this is an alternative method to the network shift but is dependent on the specific elastic Earth model (Love numbers) used in (3).

[18] Blewitt *et al.* [2001] did not provide details on how they realized the CF frame which led Wu *et al.* [2002] to incorrectly assume that the results of Blewitt *et al.* [2001] were biased by using Love numbers in the CF frame rather than the CN frame. In fact, Blewitt *et al.* [2001] used a stochastic approach [Davies and Blewitt, 2000] for implicit estimation of translation parameters, which can be shown [Blewitt, 1998] to be equivalent to explicit estimation using the functional model:

$$[\Delta\mathbf{s}_i]_{\text{OBS}} = \mathbf{t} + \mathbf{G}^T \text{diag} [[l'_1]_{\text{CF}} [l'_1]_{\text{CF}} [h'_1]_{\text{CF}}] \mathbf{G} \frac{\rho_s}{\rho_E} \begin{pmatrix} T_{11}^C \\ T_{11}^S \\ T_{10}^C \end{pmatrix} \quad (5)$$

In this approach the frame-dependent choice of degree-1 Love numbers used in (3) is inconsequential, because the translation parameter \mathbf{t} ensures no-net translation of the network, thus the CN frame is realized. The design matrix for this deformation approach is given in Appendix A.

[19] This approach has the advantage that it is not subject to errors due to approximating $\Delta\mathbf{r}_{\text{CF-CM}}$ with $\Delta\mathbf{r}_{\text{CN-CM}}$ as in the network shift, and errors in the GPS determination of CM (orbit errors) which map equally (i.e., as a translation) into all site displacements are removed by the translation in (5). Removing common mode errors in site displacements by estimating a Helmert transformation and expressing displacements in a CN frame is common in GPS analysis [Davies and Blewitt, 2000; Heflin *et al.*, 2002; Wdowinski *et al.*, 1997]; however, the residual displacements had not been previously used to estimate degree-1 coefficients of the load. The results are still subject to errors due to the ignored higher degrees in (1) [Wu *et al.*, 2002] and GPS observational errors not common to all sites; both errors are of course network dependent.

[20] Dong *et al.* [2003], Wu *et al.* [2003], and Gross *et al.* [2004] extended this approach to estimate coefficients of the load up to degree 6 using equivalent forms of (1). Such an approach should reduce the errors in the estimate of degree 1 which may exist in the estimates of Blewitt *et al.* [2001] caused by ignoring the higher degrees [Wu *et al.*, 2002]. Additionally, estimating higher-degree terms requires a dense and well-distributed network.

[21] In their estimation procedure both Dong *et al.* [2003] and Wu *et al.* [2003] place their observations in the CN

frame by first removing a seven parameter Helmert transformation and estimating loading coefficients from the residuals. Both these results could be biased downward because of the inclusion (and subsequent removal from the displacements) of a scale parameter.

3. GPS Error Analysis

[22] In order to fully test the different techniques for estimating geocenter motion we first investigate the likely error sources involved. Errors are highly network dependent so it is crucial to considering different (but realistic) networks. The likely errors naturally fall into two categories: random and systematic GPS technique-specific errors and systematic errors due to mismodeling of the loading deformation. Random errors are considered in section 3.3 by propagation of the GPS formal error. The systematic effects of mismodeling are considered in section 4 by creating synthetic GPS data sets with known statistical properties so that the estimated value can be compared to the “true” value used to create the data. The effects of GPS-specific systematic errors are difficult to analyze here, orbit errors tend to affect the z component more than x or y since they are modulated by Earth rotation [Watkins and Eanes, 1994] and some degree of uncertainty in geocenter motion is attributable to not resolving ambiguities. Other GPS-specific systematic errors are also likely, such as second-order ionospheric effects [Kedar et al., 2003] and tidal aliasing [Penna and Stewart, 2003]; however, their consideration is beyond the scope of this paper and we concentrate on the systematic errors, which are generated by the loading deformation itself, because of mismodeling.

3.1. GPS Data

[23] We use global GPS data from six International GNSS Service (IGS) analysis centers over the 7-year period 1997.25–2004.25: GeoForschungsZentrum (GFZ), the European Space Agency (ESA), the NASA Jet Propulsion Laboratory (JPL), Natural Resources Canada (EMR), the US National Geodetic Survey (NGS), and Scripps Institution of Oceanography (SIO). Weekly coordinate Solution Independent Exchange (SINEX) files [Blewitt et al., 1995] from each analysis center are produced and archived each week as part of routine IGS activity. Each SINEX file contains a precise and rigorous estimate of the IGS polyhedron, using the most up-to-date methods and techniques [Blewitt et al., 1995]; the orbit, timing and coordinate products from both the IGS and individual analysis centers are used in much of the ongoing global and regional scientific GPS processing, and the analysis center solutions are a core contribution to the ITRF.

[24] Each IGS analysis center processes its own particular subset of the IGS network, using software which can have quite different approaches to determining site coordinates from GPS data. As such they provide an ideal data set for exploring the errors in geocenter motions and the best method to estimate them, since the major processing software and strategies are represented yet produce solutions from the same GPS data. Most importantly, the SINEX format allows for complete archival of estimated site coordinates, the full variance-covariance matrix and the full set of applied constraints; these constraints can be subsequently

removed to produce “loose” or “free” networks [Davies and Blewitt, 2000; Heflin et al., 1992]. This is important since we wish to assess the determination of geocenter motions free from any particular frame that the individual analysis center has chosen to represent its weekly coordinates. Once these constraints are removed, the SINEX files form GPS realizations of the CM frame.

[25] Velocities are estimated and removed from the analysis center solutions using a consistent rigorous least squares strategy with full covariance information [Davies and Blewitt, 2000; Lavallée, 2000]. Sites with less than 104 weekly observations over 2.5 years are rejected. A period of 2.5 years is chosen to eliminate velocity errors associated with annual signals [Blewitt and Lavallée, 2002]. Outliers and data segments with known problems are rejected, and offsets due to equipment changes (particularly radome and antenna changes), earthquakes, or site moves are estimated. The analysis centers ESA and SIO do not apply the pole tide correction so this is applied using IERS standards [McCarthy and Petit, 2004].

[26] To maintain a consistent level of formal error scaling, the input weight matrices are scaled by the unit variance (chi-square per degree of freedom) in the case where residuals are estimated assuming the network shift approach, which is standard in GPS analysis. It is difficult to ascertain whether formal errors will be overestimated or underestimated in this case. If unmodeled observational errors are larger than the real geophysical loading then errors will be underestimated; conversely, if the loading dominates then this approach could overestimate the errors. We take this scaling to be at least a commonly accepted approach.

3.2. Networks

[27] The estimation of geocenter motions is fundamentally linked to the representation of the Earth’s surface using a geodetic network. Network size and distribution are therefore key factors in the error assessment of different methods. The analysis centers have different approaches to choosing the weekly subset of the IGS global network they analyze. Figure 2 shows the number of sites analyzed each week after the rejections necessary to estimate the velocities mentioned in section 3.1. Some analysis centers such as EMR restrict their analysis to a small number of sites whereas SIO maintain an analysis that more closely mirrors the overall growth of the IGS network. A crude but informative way to assess network distribution, particularly in the context of geocenter motions, is to look at the percentage of sites within opposing hemispheres centered on the direction of each Cartesian axis. Figure 3 plots the percentage of sites in the hemisphere centered upon each coordinate axis, the center line at 50% represents an “ideal” equally distributed network. Although there are a number of factors, the distribution of a realistic global geodetic network is governed primarily by the ocean-land distribution (~70% of the Earth’s surface is ocean). Figure 3 clearly reflects this: The inequality between the Northern and Southern Hemispheres in the z direction is the largest, reaching up to almost 80% of sites in the Northern Hemisphere, 30% larger than the “ideal.” The inequality in the x and y directions varies up to only 15% yet there is still a noticeable tendency toward sites being located in the

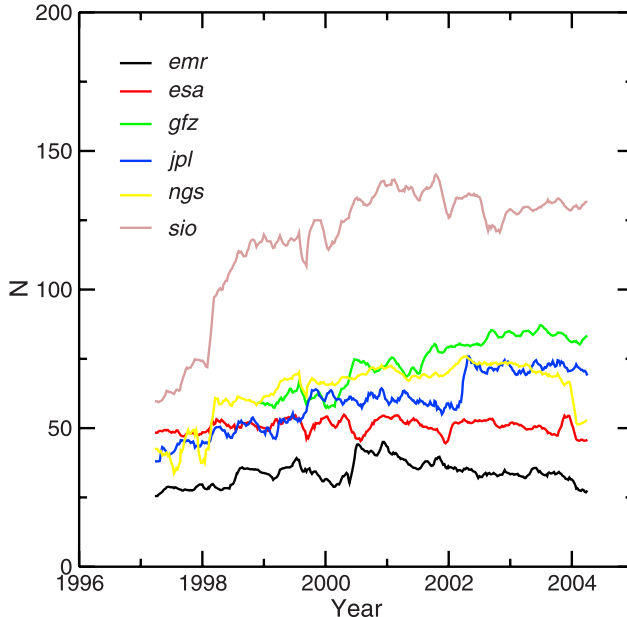


Figure 2. Number of sites in each analysis center's weekly solution for the period 1997.25–2004.25. Values are given after outlier rejection and elimination of sites with less than 104 weekly observations or less than 2.5 years of data.

hemisphere centered on the x axis (Europe) and the hemisphere centered on the negative y axis (North America). JPL maintain the best north-south distributed network in this simple analysis but only at the expense of network size. What is clear is that although the IGS network is growing considerably, the distribution is not improving at the same rate and realistically, this is always likely to be the case because of the ocean-land distribution. There is always a trade-off between reducing random error by increasing network size and possibly introducing systematic error in the geocenter motion estimates by degrading distribution. The best method for determining geocenter motions from space geodesy should therefore be able to take advantage of improved network size without necessarily better distribution.

3.3. Propagation of Observational Formal Errors

[28] Assessment of how the GPS formal errors map into each estimate is performed by propagating the formal covariance matrix of the observations to the covariance matrix of the parameters in each method. The scaling of the formal covariance matrix from each of the different analysis centers relates to the a priori variance assigned to the initial GPS phase estimate and any other scaling applied during the GPS processing, so it would be unwise to interpret the scaling of formal errors between analysis centers in detail. It is also unnecessary; it is the relative scaling, that is, the performance of each geocenter estimation method, that is of concern.

[29] Figures 4 and 5 plot the changes in formal errors over time, for two end-member cases of network size/distribution during the interval 1997.25–2004.25. The higher degrees are ignored in the degree-1 deformation and combined approaches for the time being; Table 1 lists the mean formal error over the interval for each component (x , y , and z), method, and analysis center. The strength of an

approach in dealing with different networks is reflected in the similarity between the $\mathbf{r}_{CF-CM} x$, y , and z formal error; in a robust approach the formal error on the geocenter will be the same in all directions whatever the network distribution.

[30] Figure 4 shows the formal error in the JPL geocenter x , y , and z components from each of the three methods for this interval. The formal error in all approaches reduces with time; this to some degree reflects improvements in GPS software models, but mostly reflects the increase in size of the GPS tracking network (Figure 2) which is about 100% over the entire interval. The distribution of the network (Figure 3) remains relatively well balanced and consistent over time and this is reflected in the formal errors for the network shift approach being roughly identical in x , y , and z directions (Figure 4 and Table 1). The network shift method is predicted to perform slightly better than the degree-1 deformation approach for all components. In part, this is due to dilution of precision: It is necessary to estimate three extra parameters in the degree-1 deformation approach. Of most interest is that the CM approach is predicted to give mean formal errors between 42–52% smaller than either the network shift or degree-1 deformation approaches.

[31] Figure 5 shows the formal error in the SIO geocenter x , y , and z components from each of the three methods for the same interval. The results are quite different to those of the JPL network since the SIO network includes more sites (Figures 2 and 3). In this case the most noticeable effect is

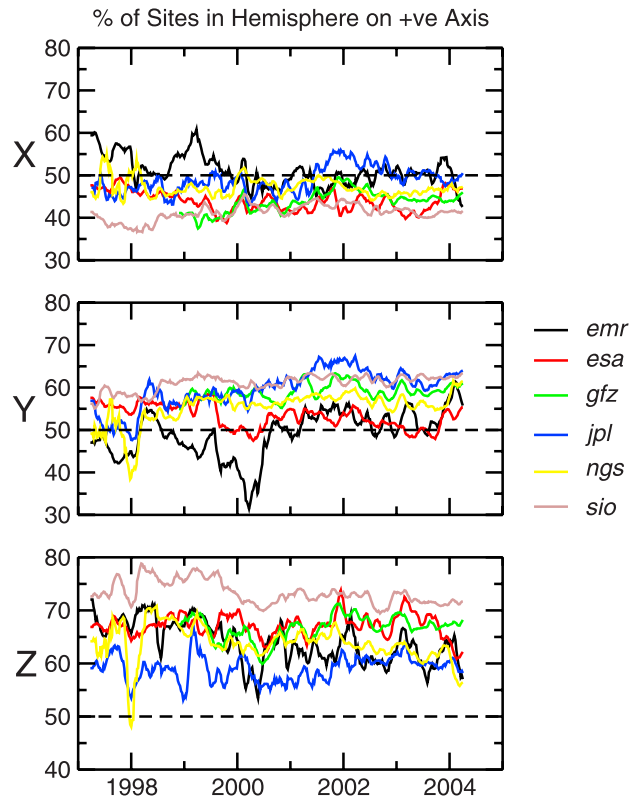


Figure 3. Percentage of all analysis center sites in the hemisphere centered on positive x , y , and z axes for the period 1997.25–2004.25. The 50% line represents the ideal situation of a well-distributed network.

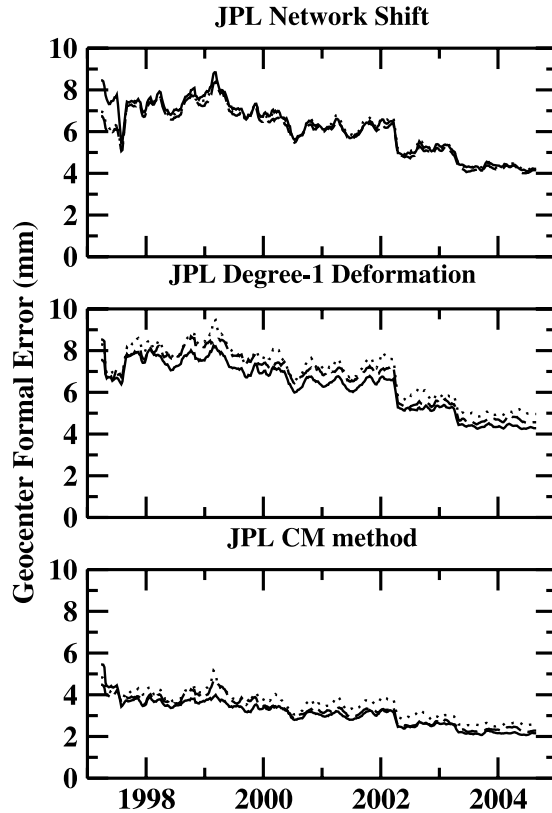


Figure 4. Jet Propulsion Laboratory geocenter formal error for the period 1997.25–2004.25. (top) Network shift method, (middle) Degree-1 deformation method, and (bottom) CM method. Formal error is plotted with (for x) a dotted line, (for y) a dashed line, and (for z) a solid line.

the poor performance of the network shift. Because of the uneven network, the z component of geocenter formal error is approximately 3 times that in the x and y (Figure 5). The degree-1 deformation approach, however, performs much better with both smaller and virtually identical formal errors in all directions (Figure 5 and Table 1). The CM approach again improves the formal errors in all directions. The improvement in mean formal error in x , y , and z is 2%, 72%, and 69%, respectively, over the degree-1 deformation approach, and 16%, 44%, and 83%, respectively, over the network shift approach.

[32] Figures 4–5 and Table 1 demonstrate that the network shift approach should perform well when a network is well distributed, in fact as well as the degree-1 deformation approach (although this does not include the error in assuming $\mathbf{r}_{\text{CF-CM}} = \mathbf{r}_{\text{CN-CM}}$ or aliasing effects), but when a network is poorly distributed, the degree-1 deformation approach should be far superior. This can explain the observation that the degree-1 deformation approach produces geocenter motions that are more stable with time [Blewitt et al., 2001; Dong et al., 2003], since the degree-1 deformation approach should perform much better as network distribution changes. The CM approach is predicted to perform considerably better than either approach (Table 1) despite the network distribution; in principle this will always be the case as the information content of both the other approaches is used. This suggests that it may be

possible to exploit the improvement in IGS network size with time despite the relatively small improvement in N-S distribution.

4. Analysis of Geocenter Motion Mismodeling Errors

4.1. Synthetic Data

[33] Synthetic GPS data are created by adding displacements predicted by a hydrological loading model to site positions specified by the analysis center networks. We use surface atmospheric pressure from the National Center for Environmental Prediction (NCEP) reanalysis data set [Kalnay et al., 1996]. The data are provided on a $2.5^\circ \times 2.5^\circ$ global grid at six hourly intervals. We average 7 days of data (28 epochs) centered on the GPS week corresponding to the SINEX files. The ocean is treated as a pure inverted barometer; that is, we set the pressure to zero over the oceans.

[34] For the ocean bottom pressure, we use values derived from a simulation of the oceans completed at JPL as part of their involvement in the Estimating the Circulation and Climate of the Ocean (ECCO) consortium [Stammer et al., 1999]. The ocean model used in this simulation spans the globe between 77.5° south and 79.5° north latitude with a latitudinal grid-spacing ranging from $1/3^\circ$ at the equator to 1° at high latitudes and a longitudinal grid-spacing of 1° . The model is forced twice daily with wind stress and daily

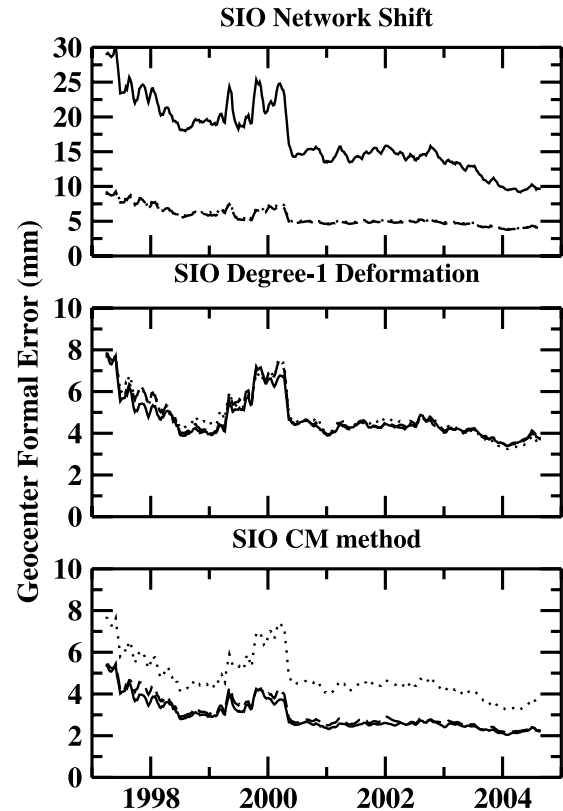


Figure 5. Scripps Institution of Oceanography geocenter formal error for the period 1997.25–2004.25. (top) Network shift method, (middle) Degree-1 deformation method, and (bottom) CM method. Formal error is plotted with (for x) a dotted line, (for y) a dashed line, and (for z) a solid line.

Table 1. Mean Geocenter Formal Error for Period 1997.25–2004.25

Analysis Center ^a	Network Shift			Degree-1 Deformation			CM Method ^b		
	X	Y	Z	X	Y	Z	X	Y	Z
EMR	10.73	11.62	28.56	10.62	11.45	10.87	9.33	6.64	6.49
ESA	7.56	7.53	33.67	10.58	10.74	10.19	9.81	5.49	5.14
GFZ	6.26	6.18	6.85	6.47	7.56	7.24	3.22	3.78	3.56
JPL	6.12	5.96	6.20	6.97	6.67	6.31	3.51	3.23	3.09
NGS	11.65	11.29	33.41	9.82	9.60	9.15	9.35	6.78	6.25
SIO	5.68	5.52	16.90	4.85	4.77	4.68	4.78	3.10	2.95

^aEMR is Energy, Mines, and Resources (Ottawa, Canada); ESA is European Space Agency (Paris, France); GFZ is GeoForschungsZentrum (Potsdam, Germany); JPL is Jet Propulsion Laboratory (Pasadena, California); NGS is National Geodetic Survey (Rockville, Maryland); and SIO is Scripps Institution of Oceanography (La Jolla, California).

^bCM is center of mass.

surface heat flux and evaporation-precipitation fields from the NCEP/NCAR reanalysis project. The 12 hourly data were averaged into weekly values.

[35] We use continental water storage variations derived from simulations of global continental water and energy balances, created by forcing the Land Dynamics (LaD) model [Shmakin *et al.*, 2002] with estimated atmospheric variables. The water storage data (snow, groundwater, and soil moisture) are provided at $1^\circ \times 1^\circ$ global resolution at monthly time periods. The most recent version of the model, LaD World-Danube, extends from January 1980 to April 2004. The monthly data were linearly interpolated to weekly values.

[36] The total load is made gravitationally self-consistent and mass conserving by adding a spatially variable surface mass layer over the oceans [Clarke *et al.*, 2005]. This amplifies the annual degree-1 component of the load and also Δr_{CF-CM} by 26%, 13% and 17% in x , y , and z components, respectively (Table 2). Figure 6 and Table 2 summarize the total load. The power spectra of the model-predicted geocenter motion are plotted in Figure 6. The overwhelming majority of spectral power is at the annual frequency since geocenter motion is driven by the seasonal water cycle. A small amount of power exists at the semi-annual frequency in the z component. The variance reduction when fitting a pure annual signal to the x , y , and z total load is 65%, 70%, and 53%, respectively. This is the reason that most work [Bouillé *et al.*, 2000; Chen *et al.*, 1999; Dong *et al.*, 1997; Dong *et al.*, 2003; Moore and Wang, 2003] concentrates on the annual component of geocenter motion and if only to avoid plotting a very large number of time series we also consider the annual signal for intercomparison purposes.

[37] A synthetic loading deformation data set is produced for each analysis center by creating correlated Gaussian normal deviates with a mean centered on the predicted deformation and variance-covariances obtained from the full

weekly SINEX formal covariance matrices. We assume that the SINEX covariance matrices represent a reasonable assessment of the random errors and a much better approximation than uncorrelated errors with a blanket value for the noise in each east, north, and up component. The synthetic data set now includes specified random errors and can be used to investigate how the random errors expected in Δr_{CF-CM} (section 3.3) combine with systematic effects from mismodeling and site network distribution.

4.2. Errors Due to Approximation of r_{CF-CM} With r_{CN-CM}

[38] The network shift approach will always be sensitive to systematic error so long as the satellite-tracking network incompletely samples the Earth's surface. The size of this error depends on the network distribution and observational errors: Wu *et al.* [2002] estimate this error for the 30-site SLR network of Bouillé *et al.* [2000] to be approximately 1 mm; Dong *et al.* [2002] also find this error to be

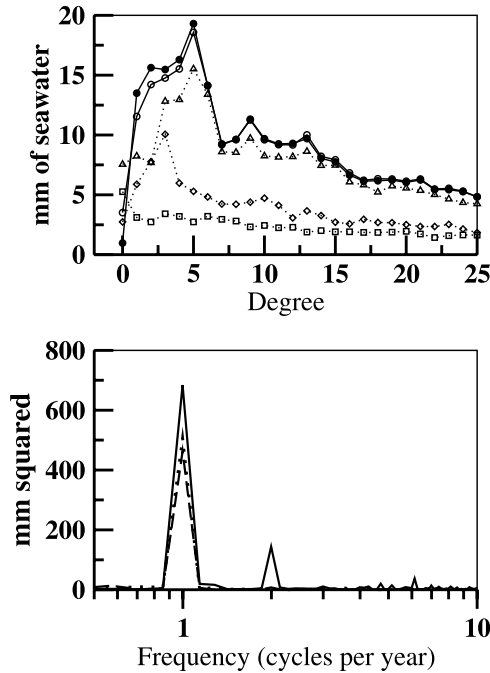


Figure 6. (top) Normalized square root annual load degree amplitudes in mm of seawater. (squares) Ocean load; (diamonds) Atmosphere; (triangles) Continental water; (open circles) Total load; and (closed circles) Equilibrated total load. (bottom) Power spectra of equilibrated total load model predicted Δr_{CF-CM} variations.

Table 2. Annual Amplitude and Phase of Load Model Used to Create Synthetic Geodetic Loading Data^a

Model	Δr_{CF-CM} Annual Amplitude ^b , mm			Δr_{CF-CM} Annual Phase, deg		
	X	Y	Z	X	Y	Z
Atmosphere	0.35	1.37	1.02	159	170	154
Continental water	0.80	0.73	2.39	234	103	255
Ocean bottom pressure	0.92	0.38	0.10	197	201	78
Total load	1.86	2.00	2.33	205	157	229
Equilibrated total load	2.35	2.25	2.72	207	160	231

^aAmplitude and phase are defined by $A \cos [2\pi(t - t_0) - \Phi]$ where t_0 is 1 January.

^bCF is center of figure; CM is center of mass.

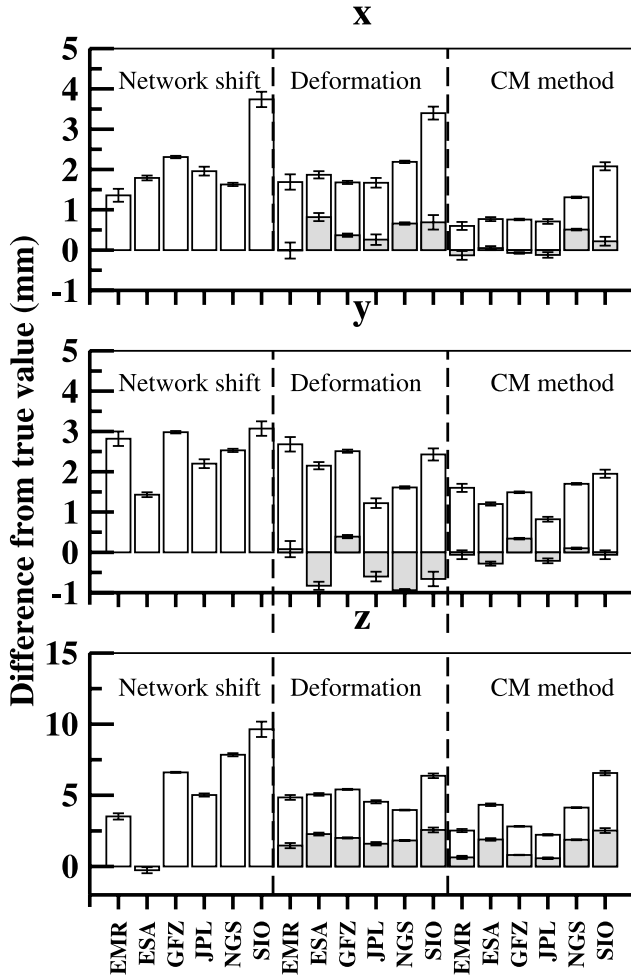


Figure 7. Histogram of Δr_{CF-CM} annual amplitude differences (mm) between those estimated from synthetic data and true value used to create the data. Shaded bars indicate that in addition to degree-1 deformation, degree-2 deformations were also estimated. Error bars are 1 standard deviation.

submillimeter. In both cases uncorrelated errors are assumed. While 1 mm is still significant when the modeled signal is on the order of 3–4 mm [Chen et al., 1999; Dong et al., 1997; Moore and Wang, 2003], assuming uncorrelated errors is likely to seriously underestimate the error when estimating the mean site displacement if real correlations exist. We compute this error for each analysis center network series using correlated synthetic data. The results are plotted in Figures 7 and 8 and discussed in section 4.4.

4.3. Errors Due to Higher Degrees of Loading

[39] The degree-1 deformation and CM approaches are not subject to errors in approximating r_{CF-CM} with r_{CN-CM} since the deformation is modeled at each site (i.e., in the CN frame); however, only the degree-1 deformation is modeled, and degrees >1 are ignored. Ignoring these higher degrees could cause significant aliasing into the estimated geocenter motion [Wu et al., 2002]. Wu et al. [2002] conduct a sensitivity analysis to estimate geocenter motion annual amplitude and consider uncertainties for the 66-site network

of Blewitt et al. [2001] to be (9, 8, 10) and (3, 2, 9) mm in x , y , and z , respectively, for two different load scenarios. Wu et al. [2002] scaled the degrees 2 to 50 coefficients in their load scenarios by 6.6, the load moment z component of Blewitt et al. [2001]. Wu et al. [2002] may have overestimated the effects of aliasing with such a scaling, especially since the load moment results of Blewitt et al. [2001] were likely already aliased.

[40] We compute the aliasing error for each analysis center network series, the degree-1 deformation and CM approaches using the correlated synthetic data. The results are plotted in Figures 7 and 8 and discussed in section 4.4.

4.4. Results

[41] Estimates of the two mismodeling errors discussed in sections 4.2 and 4.3 are plotted alongside each other in Figures 7 and 8; values estimated from the synthetic data sets are compared with the “true” values used to create the data. This way the systematic errors introduced in the network shift approach by approximation of CF with CN can be contrasted with the systematic errors introduced in the degree-1 deformation and CM approaches by higher-degree aliasing. Observational random errors (section 3.3)

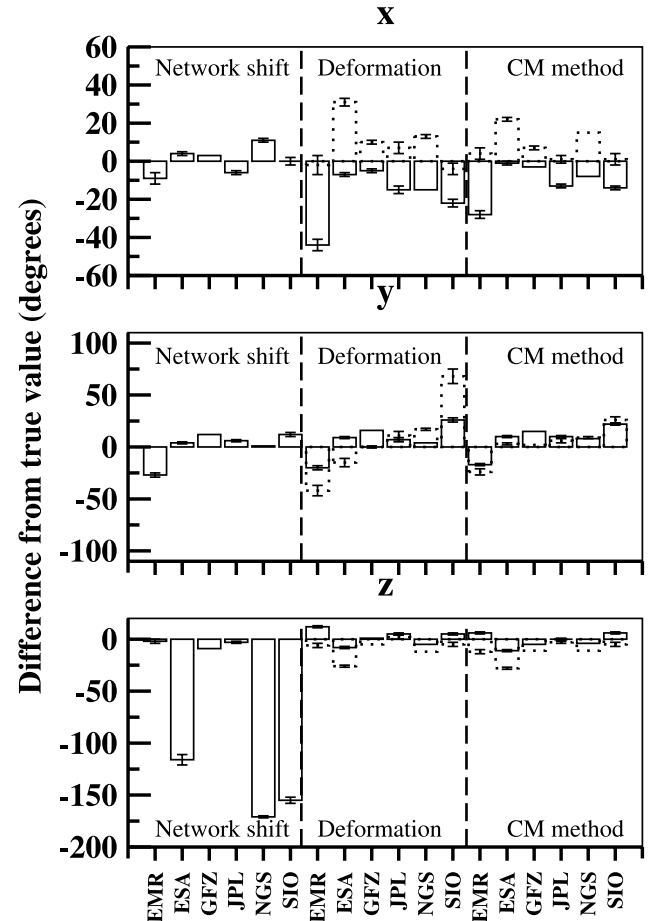


Figure 8. Histogram of Δr_{CF-CM} annual phase differences (degrees) between those estimated from synthetic data and true value used to create the data. Dotted bars indicate that in addition to degree-1 deformation, degree-2 deformations were also estimated. Error bars are 1 standard deviation.

are the same for all methods as they are specified by the synthetic data.

[42] Previous work with uncorrelated synthetic data [Dong *et al.*, 2002; Wu *et al.*, 2002] suggests that annual mismodeling errors are on the order of ~ 1 mm for the network shift approach and up to ~ 6 mm in the degree-1 deformation approach; similar results have been obtained with uncorrelated data by the authors of this paper. Such results can, however, be misleading, since global GPS solutions will have correlated random errors. If we look at our synthetic data set where intersite correlations are considered (Figures 7 and 8), a very different picture emerges; in this case, network shift annual amplitude can vary from the true value by as much as ~ 4 mm in x and y , up to 10 mm in z , and between analysis centers by almost as much. The phase variations are even more extreme with some phases shifted almost 180° from both the true value and between analysis centers. These results indicate that correlated errors in global geodetic solutions could cause significant errors and disagreement between estimates of geocenter motion when using the network shift approach (particularly when using different networks); this error is much larger than aliasing effects in the deformation approach. This conclusion is enhanced by the poor agreement between GPS geocenter motion estimates using the network shift approach [Boucher and Sillard, 1999] and observations that the degree-1 deformation approach produces more stable results [Dong *et al.*, 2003].

[43] The degree-1 deformation method produces better results than the network shift approach (Figures 7 and 8), with annual amplitudes that are generally closer to the true value and in better agreement between different networks (particularly in z). The improvement in phase stability is quite considerable. Aliasing of higher degrees still has an effect, and the best degree-1 deformation results are achieved when degree 2 is also estimated; in this case, errors are up to 0.8, 0.9, and 2.6 mm in x , y , and z amplitudes, respectively; in phase, errors are up to 31° , 42° , and 26° , respectively.

[44] The CM method consistently produces results which are closer to the true value than are either the network shift or degree-1 deformation approaches (Figures 7 and 8). When degree 2 is also estimated, amplitude errors are predicted to be up to 0.5, 0.3, and 2.5 mm in x , y , and z , respectively; if the network is well distributed, then the error in z can be as low as 0.6 mm. Phase errors are predicted to be up to 22° , 26° and 28° in x , y , and z , respectively. The method is in principle the best way to model the observations and from this simulated analysis is indeed the best performer.

[45] It can be observed that for all methods the SIO network produces results in amplitude and phase that are usually furthest from the true value, particularly when degree 2 is not estimated. This network contains a large number of regional sites and demonstrates the effects of a very uneven network. It is unlikely that such sites would normally be included in a geocenter estimation analysis; however, inclusion of these sites provides a useful end-member estimate of the errors. For such a large network it is possible to estimate spherical harmonic degrees greater than 2 with the deformation approaches [Wu *et al.*, 2003]. Only the SIO network is really large enough to do this reliably

(Figure 2). We estimate up to degree 6 with the degree-1 deformation approach and CM approach from the synthetic data; in this case, we find that the annual x and y amplitudes do not get any closer to their true values compared to the case when only degrees 1 and 2 were estimated, but the SIO z amplitudes now vary from the true value by only 0.4 mm, an improvement of 84%, with the annual phase hardly affected. This suggests that, while aliasing from degrees beyond 2 is minimal for x and y , the tendency for an uneven network in the z direction requires higher degrees to be estimated to overcome aliasing and that this may be a viable approach for large but regionally dense networks such as SIO.

5. Network Scale

[46] It is common when estimating Helmert transformations to estimate a scale parameter [Heflin *et al.*, 2002]. In the case of an uneven network this scale parameter could absorb some of the real deformation due to surface mass loading and is unnecessary when geocenter motions are estimated. This effect has been found significant for the network shift approach with noise-free, uncorrelated synthetic site data from just atmospheric pressure loading [Tregoning and van Dam, 2005]. The effect on the estimated $\Delta\mathbf{r}_{\text{CF-CM}}$ of including a scale parameter is investigated here, for correlated and noisy synthetic data from the entire surface load and additionally real GPS data.

[47] With the synthetic data, estimating scale has the largest effect on $\Delta\mathbf{r}_{\text{CF-CM}}$ estimated using the network shift approach. This effect is very significant in the z component; the annual amplitude is altered by up to 0.33, 0.16, and 1.5 mm in x , y , and z components, respectively. When using either of the deformation approaches the z component changes only up to 0.4 mm, phase differences are at most 3° for x and y with a network shift z value of 10° .

[48] For the real data the picture is very similar: The effect on the estimated $\Delta\mathbf{r}_{\text{CF-CM}}$ is significant with a maximum effect on annual amplitude of 1.29 mm in x , 2.11 mm in y , and 4.6 mm in z . These differences are again maximal for the network shift approach; for the unified approach the maximum effect is 0.86, 0.81, and 3.23 mm in z . The effect on annual phase can reach 68° in x with the network shift method.

[49] The size of the estimated scale parameter is also significant. In the synthetic data, there is no true scale variation, only scale error arising through the interaction between loading and network geometry. Figure 9 plots the power spectra of the scale series estimated for each method (network shift, degree-1 deformation, etc.), averaged over all analysis centers. The averaging is simply for clarity; the same observations are made from each individual analysis center scale spectrum. In the synthetic data (Figure 9a) the scale series power spectrum is flat with a sharp peak at the annual frequency; this is largest (and significant at 5%) for the network shift approach and gets progressively smaller (and no longer significant) when using the degree-1 deformation and CM approaches. If degree 2 is included in these latter methods then it gets smaller still. Figure 9b also plots the power spectra of the scale estimated from the real data; there is a clear annual peak which is largest for the network shift approach and reduces in amplitude when increasing

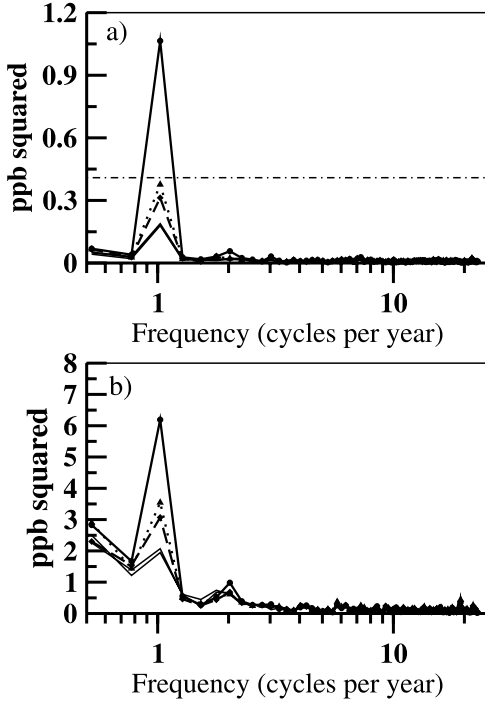


Figure 9. Average power spectra of estimated scale (a) for synthetic GPS data and (b) for real GPS data. Scale estimated with (topmost solid line) network shift approach, (dotted line) degree-1 deformation, and (dashed line) the CM method. Two lowermost solid lines in both plots are the degree-1 and CM deformation approaches where degree 2 is also estimated. Horizontal dash-dotted line in Figure 9a is 5% significance level assuming background white noise with a variance estimated from background spectra.

amounts of the loading deformation are estimated. The mean amplitude of seasonal scale estimated from the network shift approach is 0.15 ppb for the synthetic data and 0.37 ppb for the real data. It is likely that the observed seasonal changes in scale of 0.37 ppb and other results on the order of 0.3 ppb [Heflin *et al.*, 2002] are due to aliasing of the loading signal. It is encouraging to realize that the seasonal signals observed in GPS scale are at least partly due to a real loading signal rather than any particular GPS specific systematic error.

[50] Another possible scale error exists when results are put in the CN frame using a seven parameter Helmert transformation and then the residuals are used to estimate the deformation due to surface loading with the degree-1 deformation approach [Dong *et al.*, 2003; Wu *et al.*, 2003]. In this scenario it is possible that the estimation and subsequent removal from the data of a scale parameter could also remove some actual deformation due to loading. We estimate the size of the error in geocenter motions estimated this way from the synthetic data to be up to 1.84 mm in annual amplitude and up to 40° in phase. With the real data, using such a two-step procedure can change the estimates by as much as 4.3 mm in annual amplitude and 85° in phase. The effect of this two-step approach is generally to reduce load amplitude since some of the power is absorbed by the scale parameter; It is likely that this

accounts for the significant reduction in annual degree-1 amplitude observed by Dong *et al.* [2003] compared to Blewitt *et al.* [2001].

6. Comparison of Estimated Geocenter Motion

[51] Geocenter motions for the period 1997.25–2004.25 are estimated from the GPS solutions for each of the six IGS analysis centers. Annual amplitude and phase are shown in Figures 10 and 11; for comparison the predicted values from the loading model are also given. Comparing these solutions gives insight into both network and modeling effects; each analysis center has used the same GPS data but sometimes very different networks, analysis software, and procedures. The most noticeable result of this analysis is the large disagreement between analysis centers in geocenter motion annual phase for the network shift approach z component (Figure 11), this can be as large as 166° and apart from one comparison is always greater than 50°. Such a situation is

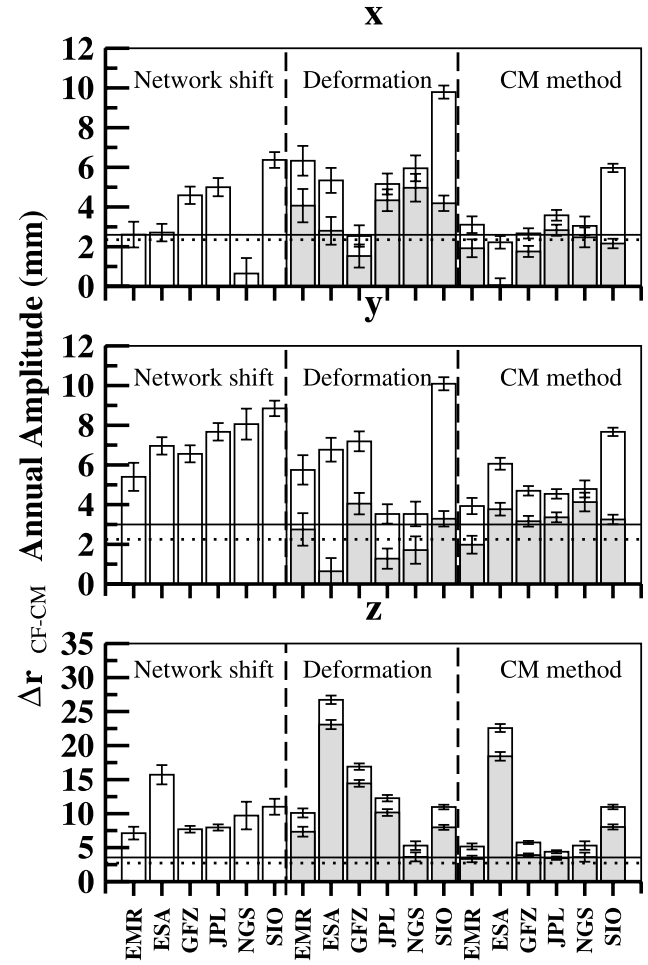


Figure 10. Histogram of GPS-estimated Δr_{CF-CM} annual amplitude (mm). Shaded bars indicate that in addition to degree-1 deformation, degree-2 deformations were also estimated. Error bars are 1 standard deviation. Solid horizontal lines are mean satellite laser ranging (SLR) estimates discussed in text. Dotted horizontal lines are equilibrated load model predicted values of Δr_{CF-CM} annual amplitude.

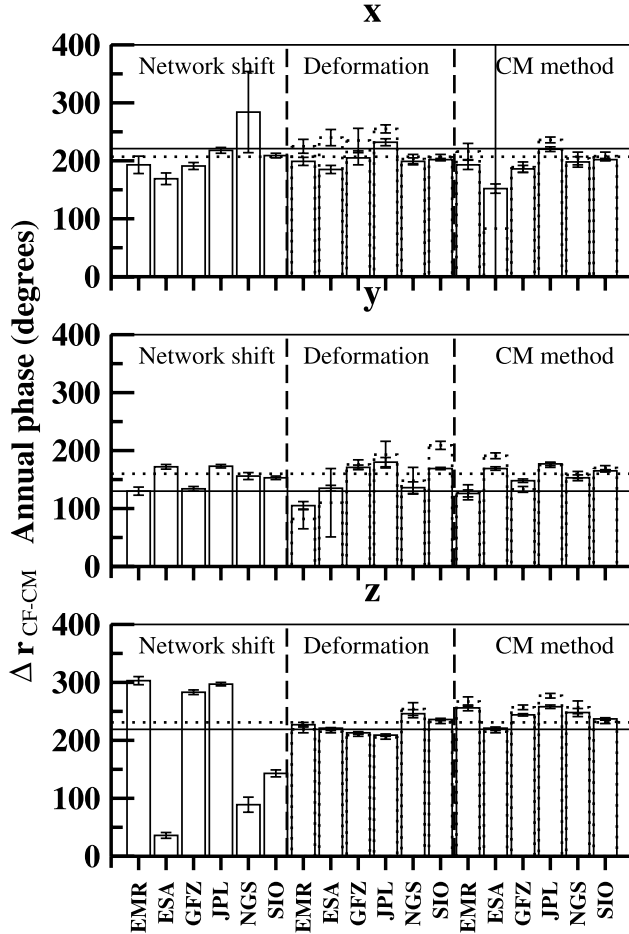


Figure 11. Histogram of estimated Δr_{CF-CM} annual phase (degrees). Dotted outline bars indicate that in addition to degree-1 deformation, degree-2 deformations were also estimated. Error bars are 1 standard deviation. Solid horizontal lines are mean SLR estimates discussed in text. Dotted horizontal lines are equilibrated load model predicted values of Δr_{CF-CM} annual phase.

predicted by the simulated data (section 4.4, Figure 8) and results from a very uneven network in the z direction. This result combined with that from the synthetic analysis clearly explains the disagreement previously seen amongst GPS estimated geocenter motions using the network shift approach [Boucher and Sillard, 1999]. Furthermore it suggests serious shortcomings in the network shift approach for estimating geocenter motions from GPS. In addition to network effects one possible explanation is the different strategies taken to ambiguity fixing; however, only JPL resolves all ambiguities; the other analysis centers fix some or none at all and no consistent differences are observed in Figures 10 and 11.

[52] The two deformation methods give considerably better agreement in phase (Figure 11); in fact, the estimates of annual phase from these methods appear to be much less affected by aliasing, network size, and distribution than is the estimated annual amplitude, another result predicted by the simulated data analysis. The weighted root-mean-square (WRMS) annual phase values (about the weighted mean) are around 15° in all components for the CM and

Table 3. Mean and Weighted RMS Estimated Analysis Center Δr_{CF-CM} Annual Amplitude and Phase for Period 1997.25–2004.25^a

Δr_{CF-CM} Annual Amplitude, mm			Δr_{CF-CM} Annual Phase, deg		
Mean	σ	WRMS	Mean	σ	WRMS
<i>All Analysis Centers, Network Shift</i>					
x	4.28	0.2	1.8	205	3
y	7.45	0.2	1.1	158	2
z	8.35	0.3	2.0	235	2
<i>All Analysis Centers, Degree-1 Deformation Method Plus Degree 2 of Total Load</i>					
x	3.71	0.2	1.2	221	3
y	2.52	0.2	1.3	183	5
z	10.59	0.2	5.7	215	1
<i>All Analysis Centers, CM Method Plus Degree 2 of Total Load</i>					
x	1.93	0.1	0.9	218	3
y	3.30	0.1	0.5	166	2
z	5.05	0.1	3.8	234	1
<i>All Analysis Centers Except ESA, Network Shift</i>					
x	4.68	0.2	1.9	208	3
y	7.57	0.2	1.3	155	2
z	8.01	0.3	1.0	270	2
<i>All Analysis Centers Except ESA, Degree-1 Deformation Method Plus Degree 2 of Total Load</i>					
x	3.82	0.2	1.2	220	3
y	2.76	0.2	1.2	184	5
z	9.20	0.2	3.6	214	1
<i>All Analysis Centers Except ESA, CM Method Plus Degree 2 of Total Load</i>					
x	2.23	0.1	0.4	218	3
y	3.21	0.1	0.5	161	2
z	4.33	0.1	1.8	251	2
<i>Analysis Centers ESA and SIO Excluded, Network Shift</i>					
x	3.93	0.3	1.7	206	4
y	6.98	0.3	1.0	156	2
z	7.80	0.3	0.5	287	2
<i>Analysis Centers ESA and SIO Excluded, Degree-1 Deformation Method Plus Degree 2 of Total Load</i>					
x	3.57	0.3	1.6	231	5
y	2.44	0.3	1.4	161	7
z	9.93	0.3	4.5	210	1
<i>Analysis Centers ESA and SIO Excluded, CM Method Plus Degree 2 of Total Load</i>					
x	2.26	0.2	0.6	221	4
y	3.20	0.2	0.6	157	3
z	3.63	0.2	0.3	266	3
<i>All Analysis Centers Except ESA, Degrees up to 6 Estimated for SIO, Degree-1 Deformation Method Plus Total Load</i>					
x	2.55	0.2	1.6	231	4
y	2.90	0.2	1.0	176	4
z	8.80	0.2	4.2	211	2
<i>All Analysis Centers Except ESA, Degrees up to 6 Estimated for SIO, CM Method Plus Total Load</i>					
x	2.10	0.2	0.6	222	4
y	3.23	0.1	0.5	163	2
z	3.86	0.2	0.8	257	2

^aAmplitude and phase are defined by $A \cos [2\pi(t - t_0) - \Phi]$ where t_0 is 1 January. CF is center of figure; CM is center of mass. SIO is Scripps Institution of Oceanography.

degree-1 deformation methods compared with 15° , 17° and 108° in x , y , and z for the network shift method (Table 3).

[53] In Figure 10 the solution for ESA is in disagreement with the other analysis centers for all approaches; the reason for this is unknown. If we treat this solution as an outlier and exclude it, then annual amplitude agreement between the remaining five analysis center solutions is much improved (Table 3).

[54] The deformation methods are affected by aliasing. If degree 2 is also estimated then the deformation methods perform much better in amplitude as predicted by the simulated results, particularly for the large network SIO (Figure 10). The SIO network is very unevenly distributed, not normally a choice for estimating geocenter motions or defining a frame. If we restrict ourselves to “reasonable” networks only (the remaining four analyses), then the network shift method gives WRMS amplitude variation of around 1.5 mm and the degree-1 plus degree-2 method has a larger z agreement, but by far the best performance is achieved when using the CM + 2 approach: WRMS variation is entirely submillimeter at 0.6, 0.6, and 0.3 mm in x , y , and z (Table 3). In this context “reasonable” means that clustering in one axis-centered hemisphere is limited to less than 70% of sites (Figure 3).

[55] The simulated analysis (section 4.4) and *Wu et al.* [2003] suggest that estimating additional higher degrees of the load may overcome the problems of an uneven network. We estimate degrees 1 through 6 for the SIO network. In this case, the WRMS variation in x , y , and z amplitude is 0.6, 0.6, and 0.8 mm for the CM approach (Table 3). These results suggest that estimating higher degrees in the CM frame is a valid approach to take for large unevenly distributed networks; it performs almost as well as when using evenly distributed networks and just estimating degrees 1 and 2. Table 3 also suggests that modeling higher-degree deformations in the CM rather than CN frame gives improved results. Removing higher-degree deformations using GRACE results [*Davis et al.*, 2004] is another approach that may improve geocenter estimates; however, this would not be possible prior to 2002. In section 2.1 it was stated that the CM method reduces to the network shift method in the case of a diagonal or block diagonal weight matrix. This is easily verified and has been done for the results presented here; the CM and network shift methods produce near identical results in this case.

[56] The estimated annual amplitude and phase are compared with those predicted by the load model (section 4.1). Horizontal dotted lines representing the load model values are included in Figures 10 and 11, and the mean estimated values in Table 3 can be compared with the loading model predicted values in Table 2. In this comparison the CM method where degree 2 is also estimated is in best agreement with the loading model; consistently, the annual amplitude and phase are closer to that predicted by the loading model than any other method, whether SIO is included or not (still treating ESA as an outlier). Excluding SIO and ESA, agreement of the weighted mean annual amplitude with the load model is 0.09, 0.95, and 0.91 mm. If degrees up to 6 are estimated from SIO then the results are only slightly different (Table 3). Phase differences with the load model are 14° , 3° , and 35° in x , y , and z , respectively. These difference are much larger than our formal errors

(Table 3); however, if only because of aliasing, the formal errors are obviously too small. An improved estimate of the observational errors comes from the WRMS agreement between the analysis center values (Table 3). In this case the load model falls within 2 standard deviations of the CM approach best estimate (mean of four analysis centers).

[57] The annual amplitude and phase are also compared to network shift results from SLR tracking of LAGEOS 1 and 2 [*Bouillé et al.*, 2000; *Chen et al.*, 1999; *Cretaux et al.*, 2002; *Moore and Wang*, 2003]. The four SLR results are in very good agreement with a mean annual amplitude of 2.60, 3.00, and 3.55 mm, mean phase of 221° , 130° , and 219° , RMS amplitude of 0.56, 0.86, and 0.66 mm, and RMS phase of 13° , 11° , and 5° in x , y , and z , respectively. Compared to the best estimates from GPS using the CM + 2 approach (Table 3) SLR has near identical annual amplitude RMS but half that achieved by GPS in annual phase RMS. It is clear that the SLR results do not have the same errors in the network shift as GPS; the improved sensitivity of LAGEOS 1 and 2 to the geocenter means the combination of observational and approximation errors (CF with CN) are smaller. The systematic error from approximating CF with CN still exists, however, and, since the SLR tracking network does not vary to the degree GPS does, is likely similar between estimates. The CM approach could improve SLR geocenter estimates still further.

[58] The mean SLR result is plotted on Figures 10 and 11, differences between the mean SLR estimate, the best GPS mean estimate (CM + 2) and the loading model are insignificant at 2 sigma when the RMS is used as an estimate of formal error. At the 1 sigma level, there is a significant discrepancy between the geodetic measurements (which agree) and the load model in z amplitude, and the y annual phase from SLR is significantly different from both GPS and the load model.

[59] The considerably improved precision of the CM approach is still not small enough to reliably discriminate between different load models; however, the level of agreement between geodetic estimates of geocenter annual motion (Table 3) is now about the same level as that between different load models, a considerable improvement in observational precision over that previously seen from GPS.

7. Conclusions

[60] Historically, the “network shift” approach has been the most commonly used approach to estimating geocenter motions from geodetic data. We find that it has a number of shortcomings when applied to GPS. Estimated and predicted results from synthetic data demonstrate that the geocenter annual phase estimated by the network shift is particularly unstable. Significant levels of seasonal scale variation observed in GPS analysis are at least in part due to the interaction of surface mass loading with a sparse geodetic network and mismodeling of the Earth’s degree-1 deformations with the network shift approach. Scale should not be estimated with geocenter motions, or biased results will be obtained.

[61] Alternative approaches for estimating geocenter motions with GPS have involved modeling the degree-1 (and sometimes higher) deformations in realizations of the CF frame [*Blewitt et al.*, 2001; *Dong et al.*, 2003; *Wu et al.*, 2003]. In terms of formal error, modeling the deformations

in this way is much more robust when networks are uneven. Aliasing from unestimated higher degrees, although important, can be alleviated by estimating the total load to degree 2, but in the case of very large unevenly distributed networks even higher degrees must be estimated.

[62] In principle, an approach that unifies both the translation and deformation aspects of geocenter motion is more complete, should take advantage of all GPS information content, and is conventional since all deformations are modeled in the CM frame. Such an approach is found to give the lowest geocenter motion formal error, smaller differences from the true value when using synthetic data, the best agreement between five different GPS analyses and the closest agreement with the geocenter motion predicted from loading models and estimated from SLR.

[63] A note of caution must be attached, however: Unless the unified (CM) method uses a full weight matrix that is obtained from simultaneous estimation of station coordinates with orbit parameters, the relative weight of information between the translation and deformation would be incorrect. For example, using the covariance matrix from precise point positioning (which fixes the orbits) would be inappropriate and would produce nearly identical, poorer results to the network shift approach.

[64] With this newest approach, provided care is taken to ensure a balanced network or higher degrees are estimated as required, we demonstrate that it is possible to estimate geocenter motions from GPS with unprecedented submillimeter levels of precision. This level of precision is still, however, insufficient to reliably discriminate between different loading models. Geocenter motion agreement between different GPS solutions is now at the same level as geocenter motion agreement between different loading models. With improved GPS error modeling and mitigation, reprocessing of older data and further placement of GPS sites in the Southern Hemisphere, a level of precision that can in the near future discriminate between load models does now appear possible.

Appendix A: Least Squares Design Matrices

A1. CM Approach

[65] Displacements are modeled completely in the CM frame using (1) and Love numbers in the CM frame. The parameter vector is

$$\mathbf{x} = \begin{pmatrix} r_x & r_y & r_z & \Delta\mathbf{r}_{CF-CM} & T_{22}^C & T_{22}^S & T_{21}^C & T_{21}^S & T_{20}^C \cdots T_{n0}^C \end{pmatrix}^T \quad (A1)$$

where r_x , r_y , and r_z are rotation parameters, $\Delta\mathbf{r}_{CF-CM}$ is the geocenter motion, and T_{nm}^{Φ} are spherical harmonic coefficients of the higher degrees (>1) of the total surface load. The choice to include higher degrees is optional. The least squares design matrix for the i th site is

$$\mathbf{A}_i = \begin{pmatrix} 0 & z & -y & \left(\frac{3}{([h'_1]_{CE} + 2[l'_1]_{CE})} - 1 \right) \\ -z & 0 & x & \left(\frac{3}{([h'_1]_{CE} + 2[l'_1]_{CE})} - 1 \right) \\ y & -x & 0 & \left(\frac{3}{([h'_1]_{CE} + 2[l'_1]_{CE})} - 1 \right) \end{pmatrix} \cdot \mathbf{G}_i^T \text{diag} \left[[l'_1]_{CM} \ [l'_1]_{CM} \ [h'_1]_{CM} \right] \mathbf{G}_i \ \mathbf{B}_i \quad (A2)$$

where \mathbf{G}_i is the 3×3 matrix that rotates geocentric into topocentric displacements (east, north, and up) about a point with latitude φ and longitude λ .

$$\mathbf{G}_i = \begin{pmatrix} -\sin \lambda & \cos \lambda & 0 \\ -\sin \varphi \cos \lambda & -\sin \varphi \sin \lambda & \cos \varphi \\ \cos \varphi \cos \lambda & \cos \varphi \sin \lambda & \sin \varphi \end{pmatrix} \quad (A3)$$

The matrix \mathbf{B}_i contains the partial derivatives for higher degrees (>1) from (1).

A2. Network Shift Approach

[66] Generally, a least squares approach is used to estimate a Helmert transformation with up to seven parameters

$$\mathbf{x} = \begin{pmatrix} t_x & t_y & t_z & s & r_x & r_y & r_z \end{pmatrix}^T \quad (A4)$$

where the parameter $\hat{\mathbf{t}} = (t_x \ t_y \ t_z)^T$ is the least squares estimate of $\Delta\mathbf{r}_{CF-CM}$ and s is an optional scale parameter; the design matrix is

$$\mathbf{A}_i = \begin{pmatrix} 1 & 0 & 0 & x_i & 0 & z_i & -y_i \\ 0 & 1 & 0 & y_i & -z_i & 0 & x_i \\ 0 & 0 & 1 & z_i & y_i & -x_i & 0 \end{pmatrix} \quad (A5)$$

A3. Degree-1 Deformation Approach

[67] In the degree-1 deformation approach the parameter vector is

$$\mathbf{x} = \begin{pmatrix} t_x t_y t_z & r_x r_y r_z & \mathbf{r}_{CF-CM} & T_{22}^C T_{22}^S T_{21}^C T_{21}^S T_{20}^C \cdots T_{n0}^C \end{pmatrix}^T \quad (A6)$$

With translation t and rotation r (which are both discarded), geocenter motion $\Delta\mathbf{r}_{CF-CM}$ and higher degrees up to degree n of the surface mass load, the design matrix is

$$\mathbf{A}_i = \begin{pmatrix} 1 & 0 & 0 & 0 & z & -y & \left(\frac{3}{([h'_1]_{CE} + 2[l'_1]_{CE})} - 1 \right) \\ 0 & 1 & 0 & -z & 0 & x & \left(\frac{3}{([h'_1]_{CE} + 2[l'_1]_{CE})} - 1 \right) \\ 0 & 0 & 1 & y & -x & 0 & \left(\frac{3}{([h'_1]_{CE} + 2[l'_1]_{CE})} - 1 \right) \end{pmatrix} \cdot \mathbf{G}_i^T \text{diag} \left[[l'_1]_{CM} [l'_1]_{CM} [h'_1]_{CM} \right] \mathbf{G}_i \ \mathbf{B}_i \quad (A7)$$

[68] **Acknowledgments.** We thank the IGS analysis centers for providing the SINEX solutions used in this work. We would like to thank Yehuda Bock, Erricos Pavlis, and Mike Watkins for constructive reviews. The authors acknowledge a Royal Society University Research Fellowship to DAL and funds from the Luxembourg government for a visit of DAL to the European Center for Geodynamics and Seismology, April–May 2004. This work was also supported in the UK by NERC grant NER/A/S/2001/01166 to PJC and in the USA by NASA Solid Earth and Natural Hazards grant SENH-0225-0008 to GB.

References

- Altamimi, Z., P. Sillard, and C. Boucher (2002), ITRF2000: A new release of the International Terrestrial Reference Frame for Earth science applications, *J. Geophys. Res.*, 107(B10), 2214, doi:10.1029/2001JB000561.
- Argus, D. F., W. R. Peltier, and M. M. Watkins (1999), Glacial isostatic adjustment observed using very long baseline interferometry and satellite laser ranging geodesy, *J. Geophys. Res.*, 104(B12), 29,077–29,093.

- Blewitt, G. (1998), GPS data processing methodology: From theory to applications, in *GPS for Geodesy*, edited by P. J. G. Teunissen and A. Kleusberg, pp. 231–270, Springer, New York.
- Blewitt, G. (2003), Self-consistency in reference frames, geocenter definition, and surface loading of the solid Earth, *J. Geophys. Res.*, **108**(B2), 2103, doi:10.1029/2002JB002082.
- Blewitt, G., and P. Clarke (2003), Inversion of Earth's changing shape to weigh sea level in static equilibrium with surface mass redistribution, *J. Geophys. Res.*, **108**(B6), 2311, doi:10.1029/2002JB002290.
- Blewitt, G., and D. Lavallée (2002), Effect of annual signals on geodetic velocity, *J. Geophys. Res.*, **107**(B7), 2145, doi:10.1029/2001JB000570.
- Blewitt, G., M. B. Heflin, F. H. Webb, U. J. Lindqwister, and R. P. Malla (1992), Global coordinates with centimeter accuracy in the International Terrestrial Reference Frame using GPS, *Geophys. Res. Lett.*, **19**(9), 853–856.
- Blewitt, G., Y. Bock, and J. Koura (1995), Constructing the IGS polyhedron by distributed processing, in *Densification of the IERS Terrestrial Reference Frame Through Regional GPS Networks*, edited by J. F. Zumberge and R. Liu, pp. 21–38, Int. GPS Serv., Pasadena, Calif.
- Blewitt, G., D. Lavallée, P. Clarke, and K. Nurutdinov (2001), A new global mode of Earth deformation: Seasonal cycle detected, *Science*, **294**(5550), 2342–2345.
- Boucher, C., and P. Sillard (1999), Synthesis of submitted geocenter time series, in *IERS Analysis Campaign to Investigate Motions of the Geocenter*, *IERS Tech. Note* 25, pp. 15–21, Obs. de Paris, Paris.
- Bouillé, F., A. Cazenave, J. M. Lemoine, and J. F. Cretaux (2000), Geocentre motion from the DORIS space system and laser data to the LAGEOS satellites: Comparison with surface loading data, *Geophys. J. Int.*, **143**(1), 71–82.
- Chen, J. L., C. R. Wilson, R. J. Eanes, and R. S. Nerem (1999), Geophysical interpretation of observed geocenter variations, *J. Geophys. Res.*, **104**(B2), 2683–2690.
- Cheng, M. K. (1999), Geocenter variations from analysis of TOPEX/POSEidon SLR data, in *IERS Analysis Campaign to Investigate Motions of the Geocenter*, *IERS Tech. Note* 25, pp. 39–44, Obs. de Paris, Paris.
- Clarke, P. J., D. Lavallée, G. Blewitt, T. van Dam, and J. M. Wahr (2000), Effect of gravitational consistency and mass conservation on seasonal surface mass loading models, *Geophys. Res. Lett.*, **32**, L08306, doi:10.1029/2005GL022441.
- Cretaux, J. F., L. Soudarin, F. J. M. Davidson, M. C. Gennero, M. Berger-Nguyen, and A. Cazenave (2002), Seasonal and interannual geocenter motion from SLR and DORIS measurements: Comparison with surface loading data, *J. Geophys. Res.*, **107**(B12), 2374, doi:10.1029/2002JB001820.
- Davies, P., and G. Blewitt (2000), Methodology for global geodetic time series estimation: A new tool for geodynamics, *J. Geophys. Res.*, **105**(B5), 11,083–11,100.
- Davis, J. L., P. Elósegui, J. X. Mitrovica, and M. E. Tamisiea (2004), Climate-driven deformation of the solid Earth from GRACE and GPS, *Geophys. Res. Lett.*, **31**, L24605, doi:10.1029/2004GL021435.
- Dziewonski, A., and D. L. Anderson (1981), Preliminary reference Earth model, *Phys. Earth Planet. Inter.*, **25**, 297–356.
- Dong, D., J. O. Dickey, Y. Chao, and M. K. Cheng (1997), Geocenter variations caused by atmosphere, ocean and surface groundwater, *Geophys. Res. Lett.*, **24**(15), 1867–1870.
- Dong, D., P. Fang, Y. Bock, M. K. Cheng, and S. Miyazaki (2002), Anatomy of apparent seasonal variations from GPS-derived site position time series, *J. Geophys. Res.*, **107**(B4), 2075, doi:10.1029/2001JB000573.
- Dong, D., T. Yunck, and M. Heflin (2003), Origin of the International Terrestrial Reference Frame, *J. Geophys. Res.*, **108**(B4), 2200, doi:10.1029/2002JB002035.
- Farrell, W. E. (1972), Deformation of the Earth by surface loads, *Rev. Geophys.*, **10**, 761–797.
- Gross, R. S., G. Blewitt, P. J. Clarke, and D. Lavallée (2004), Degree-2 harmonics of the Earth's mass load estimated from GPS and Earth rotation data, *Geophys. Res. Lett.*, **31**, L07601, doi:10.1029/2004GL019589.
- Heflin, M., and M. Watkins (1999), Geocenter estimates from the Global Positioning System, in *IERS Analysis Campaign to Investigate Motions of the Geocenter*, *IERS Tech. Note* 25, pp. 55–70, Obs. de Paris, Paris.
- Heflin, M., et al. (1992), Global geodesy using GPS without fiducial sites, *Geophys. Res. Lett.*, **19**, 131–134.
- Heflin, M., D. F. Argus, D. C. Jefferson, F. H. Webb, and J. F. Zumberge (2002), Comparison of a GPS-defined global reference frame with ITRF2000, *GPS Solutions*, **6**, 72–75.
- Kalnay, E., et al. (1996), The NCEP/NCAR 40-year reanalysis project, *Bull. Am. Meteorol. Soc.*, **77**(3), 437–471.
- Kedar, S., G. A. Hajj, B. D. Wilson, and M. B. Heflin (2003), The effect of the second order GPS ionospheric correction on receiver positions, *Geophys. Res. Lett.*, **30**(16), 1829, doi:10.1029/2003GL017639.
- Lambeck, K. (1980), *Geophysical Geodesy: The Slow Deformations of the Earth*, Oxford Univ. Press, New York.
- Lavallée, D. (2000), Tectonic plate motions from global GPS measurements, Ph.D. thesis, Univ. of Newcastle upon Tyne, Newcastle, U. K.
- Lavallée, D., and G. Blewitt (2002), Degree-1 Earth deformation from very long baseline interferometry measurements, *Geophys. Res. Lett.*, **29**(20), 1967, doi:10.1029/2002GL015883.
- Malla, R. P., S. C. Wu, and S. M. Lichten (1993), Geocenter location and variations in the Earth orientation using global positioning system measurements, *J. Geophys. Res.*, **98**(B3), 4611–4618.
- McCarthy, D. D., and G. Petit (2004), *IERS Conventions (2003)*, *IERS Tech. Note*, vol. 32, Verl. Bundesamt Kartogr. Geod., Frankfurt am Main, Germany.
- Moore, P., and J. Wang (2003), Geocentre variation from laser tracking of LAGEOS 1/2 and loading data, *Adv. Space Res.*, **31**, 1927–1933.
- Pavlis, E. C. (1999), Fortnightly resolution geocenter series: A combined analysis of LAGEOS 1 and 2 SLR data (1993–1996), in *IERS Analysis Campaign to Investigate Motions of the Geocenter*, *IERS Tech. Note* 25, pp. 75–84, Obs. de Paris, Paris.
- Penna, N. T., and M. P. Stewart (2003), Aliased tidal signatures in continuous GPS height time series, *Geophys. Res. Lett.*, **30**(23), 2184, doi:10.1029/2003GL018828.
- Ray, J. (Ed.) (1999), *IERS Analysis Campaign to Investigate Motions of the Geocenter*, *IERS Tech. Note*, vol. 25, Obs. de Paris, Paris.
- Ray, J., D. Dong, and Z. Altamimi (2004), IGS reference frames: Status and future improvements, *GPS Solutions*, **8**(4), 251–266, doi:10.1007/s10291-004-0110-x.
- Shmakin, A. B., P. C. D. Milly, and K. A. Dunne (2002), Global modeling of land water and energy balances. part III: Interannual variability, *J. Hydrometeorol.*, **3**(3), 311–321.
- Stammer, D., et al. (1999), The consortium for estimating the circulation and climate of the ocean (ECCO), *Rep. 1*, Natl. Oceanogr. Partnership Program, Washington, D. C.
- Tapley, B. D., S. Bettadpur, M. Watkins, and C. Reigber (2004), The gravity recovery and climate experiment: Mission overview and early results, *Geophys. Res. Lett.*, **31**, L09607, doi:10.1029/2004GL019920.
- Tregoning, P., and T. van Dam (2005), Effects of atmospheric pressure loading and seven-parameter transformations on estimates of geocenter motion and station heights from space geodetic observations, *J. Geophys. Res.*, **110**, B03408, doi:10.1029/2004JB003334.
- Trupin, A. S., M. F. Meir, and J. Wahr (1992), Effects of melting glaciers on the Earth's rotation and gravitational field: 1965–1984, *Geophys. J. Int.*, **108**, 1–15.
- Vigue, Y., S. M. Lichten, G. Blewitt, M. B. Heflin, and R. P. Malla (1992), Precise determination of Earth's center of mass using measurements from the global positioning system, *Geophys. Res. Lett.*, **19**(14), 1487–1490.
- Watkins, M. M., and R. J. Eanes (1993), Long term changes in the Earth's shape, rotation, and geocenter, *Adv. Space Res.*, **13**(11), 251–255.
- Watkins, M. M., and R. J. Eanes (1994), Diurnal and semidiurnal variations in Earth orientation determined from LAGEOS laser ranging, *J. Geophys. Res.*, **99**(B9), 18,073–18,079.
- Watkins, M. M., and R. J. Eanes (1997), Observations of tidally coherent diurnal and semidiurnal variations in the geocenter, *Geophys. Res. Lett.*, **24**(17), 2231–2234.
- Wdowinski, S., Y. Bock, J. Zhang, P. Fang, and J. Genrich (1997), Southern California permanent GPS geodetic array: Spatial filtering of daily positions for estimating coseismic and postseismic displacements induced by the 1992 Landers earthquake, *J. Geophys. Res.*, **102**(B8), 18,057–18,070.
- Wu, X. P., D. F. Argus, M. B. Heflin, E. R. Ivins, and F. H. Webb (2002), Site distribution and aliasing effects in the inversion for load coefficients and geocenter motion from GPS data, *Geophys. Res. Lett.*, **29**(24), 2210, doi:10.1029/2002GL016324.
- Wu, X. P., M. B. Heflin, E. R. Ivins, D. F. Argus, and F. H. Webb (2003), Large-scale global surface mass variations inferred from GPS measurements of load-induced deformation, *Geophys. Res. Lett.*, **30**(14), 1742, doi:10.1029/2003GL017546.
- Zumberge, J. F., M. B. Heflin, D. C. Jefferson, M. M. Watkins, and F. H. Webb (1997), Precise point positioning for the efficient and robust analysis of GPS data from large networks, *J. Geophys. Res.*, **102**(B3), 5005–5017.

G. Blewitt, MS 178, 1664 N. Virginia Street, University of Nevada, Reno, NV 89557-0088, USA. (gblewitt@unr.edu)

P. J. Clarke and D. A. Lavallée, School of Civil Engineering and Geosciences, Cassie Building, University of Newcastle upon Tyne, Newcastle, NE1 7RU, UK. (peter.clarke@ncl.ac.uk; d.a.lavallee@ncl.ac.uk)

T. van Dam, European Center for Geodynamics and Seismology, Rue Josy Welter 19, Walferdange, L-7256, Luxembourg. (tvd@ecgs.lu)